文章编号：1006-9941(2017)07-0570-09

Synthesis and Properties of Energetic Ionic salts Based on 3,6-Bis(1*H*-1,2,3,4-tetrazol-5-yl-amino)-*s*-tetrazine(BTATz)

LIU Qing[1], **YANG Jin**[1], **REN Ying-hui**[1], **MA Hai-xia**[1], **XU Kang-zhen**[1], **ZHANG Chao**[1], **ZHAO Feng-qi**[2], **HU Rong-zu**[2]

(1. *School of Chemical Engineering, Northwest University, Xi'an* 710069, *China*; 2. *Xi'an Modern Chemistry Research Institute, Xi'an* 710065, *China*)

Abstract: Three kinds of energetic ionic salts, dimethylaminium salt (DMAB), 1,3-propanediaminium salt (PDAB) and 1,4-butanediaminium salt (BDAB) of 3,6-bis(1*H*-1,2,3,4-tetrazol-5-yl-amino)-*s*-tetrazine(BTATz) were synthesized. The structures of DMAB, PDAB and BDAB were characterized by IR, ^{1}H NMR, ^{13}C NMR and elemental analyses. The crystal structure of PDAB was determined by X-ray single crystal diffraction. The detonation velocity (D) and detonation pressure (p) of PDAB were calculated. The thermal decomposition behaviors of DMAB, PDAB and BDAB were studied by DSC and TG-DTG. The self-accelerating decomposition temperature (T_{SADT}), the critical temperature of thermal explosion (T_b), the thermal ignition temperature (T_{TIT}) and adiabatic time-to-explosion (t_{TIAD}) were calculated. Results show that the crystal of PDAB is monoclinic, space group $C2/c$ with crystal parameters of a = 2.2699(10) nm, b = 0.5098(2) nm, c = 1.6449(6) nm, β = 93.045(15)°, V = 1.9008(13) nm^3, D_c = 1.504 g·cm^{-3}, Z=4, $F(000)$ = 912, μ = 0.127 mm^{-1}, R_1 = 0.0673 and wR_2 = 0.2002. The values of D and p of PDAB are 8862.09 m·s^{-1} and 32.15 GPa, respectively. The values of T_{SADT} of DMAB、PDAB and BDAB are 576.87 K, 511.90 K and 521.55 K, respectively, revealing that DMAB has higher thermal stability than PDAB and BDAB. DMAB, PDAB and BDAB can be used as potential energetic materials and the property of DMAB is better than that of PDAB and BDAB.

Key words: 3,6-bis(1*H*-1,2,3,4-tetrazol-5-yl-amino)-*s*-tetrazine(BTATz); ionic salt; thermal decomposition behavior; thermal safety

CLC number: TJ55 **Document code**: A **DOI**: 10.11943/j.issn.1006-9941.2017.07.007

1 Introduction

As we all known that the high-nitrogen energetic compounds derive most of their energy from the very large positive enthalpy of formation rather than from oxidation of the fuel like carbon backbone. The materials are particularly suitable for consideration in high-performance propellant applications, because of their high positive enthalpy of formation, insensitivity to impact, friction and electrostatic discharge, and low-molecular-weight reaction products.

3,6-Bis(1*H*-1,2,3,4-tetrazol-5-yl-amino)-*s*-tetrazine (BTATz) is one of the high-nitrogen energetic compounds, with nitrogen content of 79.02%, density of 1.76 g·cm^{-3}, enthalpy of formation of +883 kJ·mol^{-1}, and moderate mechanical sensitivity[1-6]. BTATz was first synthesized by Hiskey at Los Alamos National Laboratory[7], then the detailed studies have been done, such as the purification and the quantum chemistry study of BTATz[4], the burning rate measurement[8], the dissolution properties in *N*-methyl pyrrolidone and dimethyl sulfoxide[9], its metal complexes and metal salts[10-14], even as a substitute of hexogen (RDX) in the composite modified double base (CMDB) propellant formulation[15] and the decomposition reaction kinetics and thermal safety of BTATz-HNIW-CMDB propellants[16]. Many researches focused on the BTATz show that it has a prospect using as a primary component in the high burning rate propellant for the booster rocket motor and the kinetic energy ammunition, and it also can be used in the minimum signature propellant for the smokeless ammunition[14,17-19].

Generally, energetic nitrogen rich salts become the most exciting developments and continue to attract more interesting than atomically similar non-ionic analogues, due to the excellent performance of lower vapour pressures, higher heats of formation, and better thermal stability[20]. Salt formation of the acidic precursor by direct neutralization or metathesis reactions with alkaline nitrogen-rich cations is a very effective method to increase the nitrogen content, the heats of formation and the possibility to form the hydrogen bond, as a consequence of the densities and performances. Therefore, some energetic ionic salts have been reported[21-23]. For BTATz, its di-ammonium, di-hydroxylammonium, and di-hydrazinium salts had been synthesized and added into composite propellant[2,19], and the result indicates that all of them have the po-

Received Date: 2016-11-16; **Revised Date**: 2017-03-09

Project Supported: National Defense Pre-Research Foundation of China (9140A28020111BQ3401) and National Natural Science Foundation of China(21673179)

Biography: LIU Qing(1993-),female, graduate, research field: energetic materials. e-mail: 867950019@qq.com

Corresponding Author: REN Ying-hui(1977-),female, associate-professor, research field: synthesis and properties of new energetic materials. e-mail: nwuryh@163.com

tential to be a propellant component.

Herein, three novel energetic ionic salts based on BTATz (Scheme 1) with excellent physical chemistry properties were first presented with BTATz and different amine salts in the solvent of DMF. The structure of salts has been fully characterized. The differential scanning calorimetry(DSC) and thermogravimentry(TG) technique were adopted to investigate the thermal behavior at 300–800 K. Theoretical calculations predicting energetic performances were also carried out.

2 Experimental

2.1 Materials

BTATz used in this work was synthesized according to the literature method[4]. All solvents were obtained from typical commercial sources and used without further treatment.

2.2 Experimental Equipments and Conditions

A suitable crystal of PDAB was selected and its crystal structure was determined bya Bruker SMART APEXⅡ diffractometer. X-ray diffractometer using MoKa radition (λ = 0.071073 nm) graphite monochromatization. The crystal structure was solved by direct methods (SHELXTL-97), the data were revised with *L*p and empirical absorption, and F^2 was corrected with complete matrix least-squares procedure[24].

The TG and DSC curves under the condition of flowing nitrogen gas (purity, 99.999%; atmospheric pressure) were obtained by using a TA2950 thermal analyzer (TA Co., USA) and a 204HP differential scanning calorimeter (Netzsch Co., Germany). The sample mass was about 1mg at the heating rate (β) of 10 K·min^{-1} to TG-DTG experiments and the N_2 flowing rate was 40 cm^3·min^{-1}; for DSC analyses, the N_2 flowing rate was 50 cm^3·min^{-1}, the Al_2O_3 was used as reference sample and the type of crucible was aluminum pan with a pierced lid. The sample mass was about 1mg at different heating rate of 5, 10, 15 and 20 K·min^{-1}, respectively. The specific heat capacity (c_p, J·g^{-1}·K^{-1}) was determined with continuous c_p mode on a Micro-DSC III mircocalorimeter (Setaram Co., France) in the atmosphere of N_2, the reference sample was calcined *a*-Al_2O_3 and the sample mass was about 100 mg with the heating rate of 0.15 K·min^{-1}.

2.3 Synthesis and Characterization of the Salts of BTATz

The salts of BTATz were prepared via one-pot method (Scheme 1). In brief, aqueous dimethylamine (33%) /1,3-propanediamine/1, 4-butanediamine ethylenediamine (equivalent molar to BTATz) was dropwise added to 20 mL DMSO contained 2 mmol BTATz under magnetic stirring at room temperature. Then, the mixtures were heated to 333.15 K under vigorous stirring for 1 h. Upon the completion of the reaction, the red precipitate was filtered off, washed with a copious amount of ethanol to remove excessive original materials, and dried at 333.15 K at a vacuum drying oven for 3 h. The resulting compounds were donated as DMAB (dimethylaminium salt of BTATz), PDAB (1,3-propanediaminium salt of BTATz) and BDAB (1,4-butanediaminium salt of BTATz), respectively.

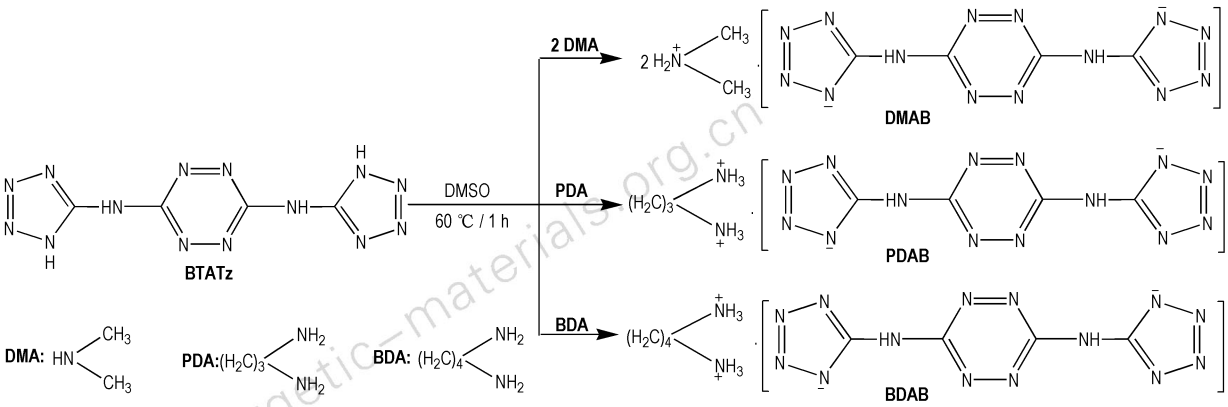

Scheme 1 Synthesis of three energetic ionic salts based on BTATz

DMAB: yeild 49.5%; IR(KBr, ν/cm^{-1}): 3241(—NH_2), 3014 (N—H), 2853, 2766 (—CH_3), 1741, 1608 (C—N), 1434 (N—N), 1046, 965, 771; elemental analysis (%) calcd for $C_8N_{16}H_{18}$: C 28.76, H 3.857, N 63.58; found: C 28.41, H 5.340, N 65.13; ^{1}H NMR (DMSO-d_6, 400 Hz) δ: 2.35 (d, *J*=18.82, —CH_3), 2.59–3.05 (m, —NH—CH_3), 3.34 (s, —NH(BTATz)); ^{13}C NMR (DMSO-d_6, 400 Hz) δ: 34.51 (s), 157.27 (s), 159.36 (s).

PDAB: yield 72.5%. IR (KBr,ν/cm^{-1}): 3435 (—NH_2), 3248 (N—H), 2967, 2793(—CH_2—), 1601, 1501(C—N), 1434 (N—N), 1046, 959, 765; elemental analysis (%) calcd for $C_7N_{16}H_{14}$: C 26.03, H 3.230, N 65.32; found: C 25.97, H 3.641, N 63.77; ^{1}H NMR (DMSO-d_6, 600 Hz) δ: 1.66–2.02 (m, —CH_2—CH_2—NH_2), 2.60–2.64 (m, —CH_2—NH_2),

2.99 (t, J=7.3Hz, —NH_2), 3.33 (s, —NH(BTATz)).

BDAB: yield 73.6%. IR (KBr, ν/cm^{-1}): 3222 (—NH_2), 2853 (—CH_2—), 2144 (—NH_3), 1655, 1581, 1494 (C—N), 1427 (N—N), 1052, 959, 724; elemental analysis (%) calcd for $C_8N_{16}H_{16}$: C 29.39, H 3.771, N 61.93; found: C 28.63, H 5.061, N 63.05; ^{1}H NMR (DMSO-d_6, 600 Hz) δ: 1.48–1.72 (m, —CH_2—CH_2—NH_2), 2.63–2.93 (m, —CH_2—NH_2), 2.93–3.59 (m, —NH_2), 3.59 (s, —NH(BTATz)).

All salts of the BTATz, which were isolated as powder materials, are non-hygroscopic and stable in air. The single crystal of PDAB suitable for X-ray determination was obtained by slow evaporation of the deionized water at room temperature. PDAB crystallizes in monoclinic $C2/c$ and crystal parameters of a = 2.2699 (10) nm, b = 0.5098 (2) nm, c = 1.6449 (6) nm, β = 93.045 (15)°, V = 1.9008 (13) nm^3, D_c = 1.504 g·cm^{-3}, Z=4, F(000) = 912, μ = 0.127 mm^{-1}, R_1 = 0.0673, wR_2 = 0.2002. The main bond length and angle are listed in Table 1, and its structure is shown in Fig. 1a. The crystal data have been deposited in CCDC with the number of 823528.

Table 1 Selected bond length and angles for the PDAB

bond	length /nm	bond	angle /(°)
N(1)—C(1)	13.33(5)	C(1)—N(1)—N(2)	104.1(3)
N(1)—N(2)	13.67(5)	N(3)—N(2)—N(1)	109.0(3)
N(2)—N(3)	12.89(4)	N(2)—N(3)—N(4)	110.8(3)
N(3)—N(4)	13.41(5)	C(1)—N(4)—N(3)	104.3(3)
N(4)—C(1)	13.37(5)	C(2)—N(5)—C(1)	128.3(3)
N(5)—C(2)	13.60(5)	N(7)#1—N(6)—C(2)	118.7(3)
N(5)—C(1)	13.75(5)	N(6)#1—N(7)—C(2)	116.6(3)
N(6)—N(7)#1	13.27(4)	N(1)—C(1)—N(4)	111.8(4)
N(6)—C(2)	13.40(5)	N(1)—C(1)—N(5)	127.3(3)
N(7)—N(6)#1	13.27(4)	N(4)—C(1)—N(5)	120.9(3)
N(7)—C(2)	13.42(5)	N(6)—C(2)—N(7)	124.7(3)
N(8)—C(3)	14.81(6)	N(6)—C(2)—N(5)	114.7(3)
C(3)—C(4)	14.95(6)	N(7)—C(2)—N(5)	120.6(4)
C(4)—C(3)#2	14.95(6)	N(8)—C(3)—C(4)	111.5(5)
		C(3)#2—C(4)—C(3)	110.7(6)

3 Results and Discussion

3.1 X-Ray Crystallography of PDAB

The results of the elemental analysis are a bit of different from the crystal structure, because the measurement state is different between two methods. The solid powder was used in the elemental analysis, while the single structure that is suitable to X-ray diffract obtained from the solvent. The analytical results indicate that there are a cation $C_3N_2H_{12}^{2+}$(1,3-propanediamine), an anion $C_4N_{14}H_2^{2-}$(BTATz^{2-}), and three crystal water molecules in one unit.

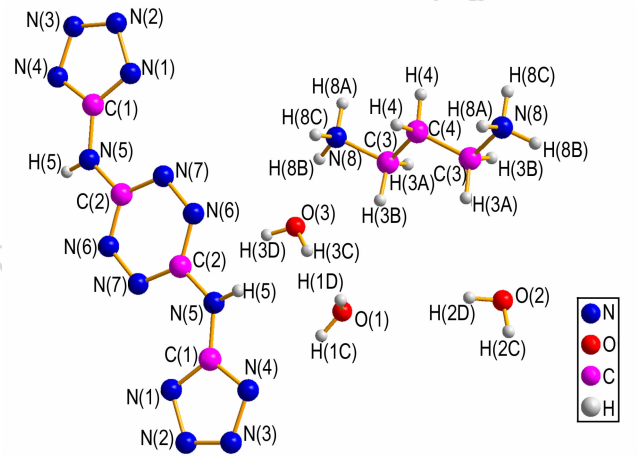

a. crystal structure

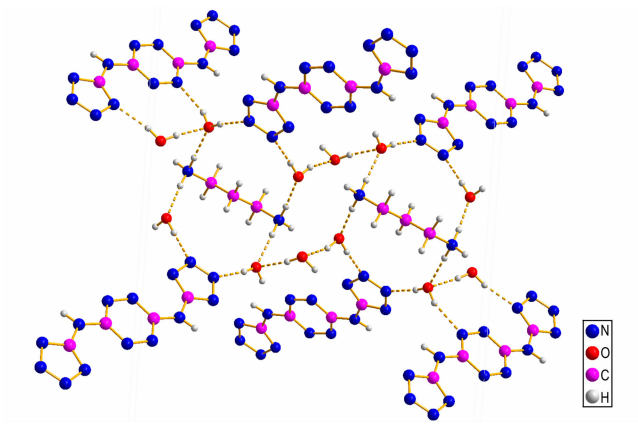

b. H-bonding interactions

Fig. 1 Crystal structure and interaction of the intermolecular hydrogen bonds for PDAB

The average bond lengths of C—N (0.1338 nm) and N—N (0.1331 nm) in tetrazine ring are shorter than the normal length of C—N (0.1450 nm), which implies the existence of conjugated action in tetrazine ring and the tetrazole ring. BTATz anion consisted by the atoms of N(1)—N(7), C(1) and C(2) shows the good coplanarity, its plane equation is as following: 15.309x–3.196y+5.819z=3.0282.

There are intermolecular N—H···O hydrogen bonds linking four water molecules, andN atom of BTATz interact to O atom of H_2O by the hydrogen bond O(2)—H(2D)···N(2) and O(1)—H(1D)···N(3). The data of hydrogen bond are shown in Table 2. Two BTATz molecules, one 1,3-propanediamine molecule and six free water molecules link by the hydrogen bond to form a ring structure. These rings are in turn linked by the intermolecular O(2)—H(2C)···O(3) and O(3)—H(3C)···O(1) hydrogen bonds to form the two-dimensional chain structure, which is shown in Fig. 1b.

Table 2 The hydrogen bond data for PDAB

D—H···A	*d*(D—H) /nm	*d*(H—A) /nm	*d*(D—A) /nm	∠DHA/(°)
N(8)—H(8C)···O(1)#1	0.0906	0.1880	0.2781	172.53
N(5)—H(5)···N(4)#2	0.0878	0.2108	0.2983	175.00
O(1)—H(1C)···N(6)#3	0.0825	0.2104	0.2899	161.97
N(8)—H(8A)···O(2)#4	0.0907	0.1943	0.2848	175.08
O(2)—H(2D)···N(2)#5	0.0835	0.2075	0.2884	163.10
O(3)—H(3D)···N(1)#6	0.0837	0.1931	0.2754	167.63
O(3)—H(3D)···N(2)#7	0.0837	0.2664	0.3343	139.25
O(1)—H(1D)···N(3)#8	0.0851	0.1903	0.2748	171.72
O(2)—H(2C)···O(3)#9	0.0827	0.2198	0.2957	152.60
N(8)—H(8B)···O(3)	0.0895	0.1956	0.2796	155.64
O(3)—H(3C)···O(1)	0.0834	0.1925	0.2748	168.40

Note: Symmetry codes: #1: *x*, *y*-1, *z*; #2: -*x*+1/2, *y*-1/2, -*z*+1/2; #3: *x*, *y*+1, *z*; #4: -*x*, *y*-1, -*z*+1/2; #5: -*x*+1/2, *y*-1/2, -*z*+1/2; #6: -*x*+1/2, -*y*+3/2, -*z*; #7: -*x*+1/2, -*y*+3/2, -*z*; #8: -*x*+1/2, *y*-1/2, -*z*+1/2; #9: *x*, -*y*+2, *z*+1/2.

3.2 Thermal Behavior and Thermal Decomposition Reaction Kinetics of BTATz Salts

The thermal behavior and decomposition character of the BTATz salts are determined by DSC and TG. Typical DSC-TG curves obtained are shown in Fig. 2.

Fig. 2a shows that there is one endothermic (435.15–507.05 K) and two exothermic processes (547.05–624.75 K, 630.25–712.65 K) in DSC curve for DMAB, which is corresponding to the two mass loss stages in TG curve. It can be inferred that the melting process overlaps with the thermal decomposition one leading to a one-step mass loss (29.20%) according to our results in Fig. 2a. A mass loss of 29.20% can be regard as the breaking of the ion bond between two N atoms and the losing of two dimethyamine ions from the system, which is near to the theory one (27.20%). The big exothermic process should be caused by the breaking of the C—N bond that connected the tetrazole and the tetrazine, and the mass loss can be identified with the loss of two tetrazole rings (63.51%), which is close to the theoretical value (64.49%).

Notably, the DSC and TG curves for the other two salts are similar to each other (Fig. 2b and Fig. 2c). There is only one exothermic process in DSC curve and one mass loss stage in TG curve. The thermal decomposition process occurs at the temperature range of 507.85–555.35 K for PDAB and 494.85–583.95 K for DBAB, the peak temperature is 530.05 K and 542.77 K, respectively. Both of them are corresponding to the mass loss of 57.23% and 34.20% in the TG curves. As a consequence, BDAP should be the ring opening of the tetrazine and the break of ion bond (theoretical value 57.02%) and BDAB maybe the ring opening of the terazine (theoretical value 32.72%). The left should be a certain product with high melt point.

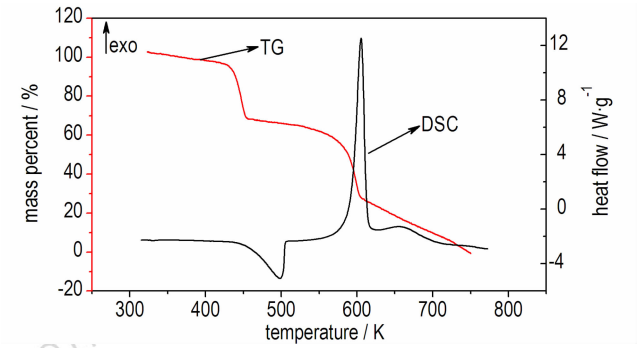

a. DMAB

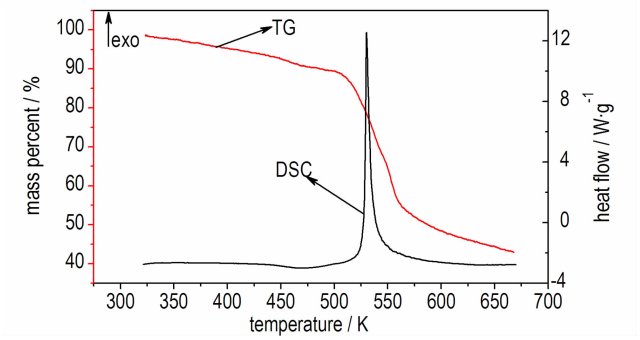

b. PDAB

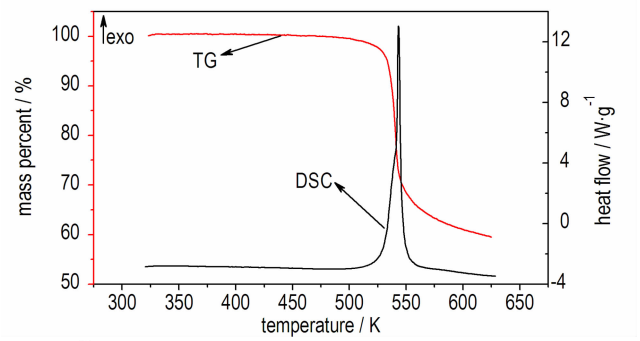

c. BDAB

Fig. 2 DSC and TG curves for different samples at a heating rate of 10 K·min^{-1}

The decomposition of explosives may be caused by the reactions in or between molecules at specific temperature. The decomposition of energetic salt composed ofcations and anions is possibly related to the nucleophilic reactions of anions or electrophilic reactions of cations.

To obtain the kinetic parameters [apparent activation energy, pre-exponential constant] and the most probable kinetic model functions of major exothermic decomposition reaction for DMAB, PDAB and BDAB, the five integral methods (General integral, MacCallum-Tanner, Šatava-Šesták, Agrawal, Flynn-Wall-Ozawa) and one differential method (Kissinger)[20, 24-25] are employed. The basic data for the main exothermic decomposition process used in calculated are listed in Table 3.

Table 3 The nonisothermal data of DMAB, PDAB and BDAB obtained by DSC curves at different heating rates

salt	β/K · min^{-1}	T_e/K	T_p/K	ΔH/J · g^{-1}
DMAB	5.0	584.55	597.35	1180
	10.0	592.75	605.45	1218
	15.0	597.65	610.35	1209
	20.0	601.45	613.85	1169
PDAB	5.0	520.85	522.15	595.9
	10.0	528.35	530.05	602.8
	15.0	532.45	534.85	625.8
	20.0	535.75	538.45	656.9
BDAB	5.0	530.71	534.55	535.7
	10.0	537.98	542.77	678.4
	15.0	541.91	547.86	663.1
	20.0	544.43	551.27	663.2

Note: T_e is the onset temperature for the main exothermal decomposition reaction in DSC curve and T_p is the peak temperature; ΔH is the decomposition heat.

The DSC curves at the heating rate of 5, 10, 15, 20 K · min^{-1} are dealt with mathematic means, and the temperature data corresponding to the conversion degrees (α) can be obtained. The values of E_a are obtained by Ozawa's method from the isoconversional DSC curves at four different heating rates, and the relation E_a-α curves of three salts are displayed in Fig. 3. As can be seen from Fig. 3, the activation energy changes slightly in the section of 0.10–0.90 (α) for DMAB, 0.20–0.80 for PDAB, and 0.10–0.50 for BDAB, so it is reliable to select the above mentioned sections to study the mechanism of the thermal decomposition reaction.

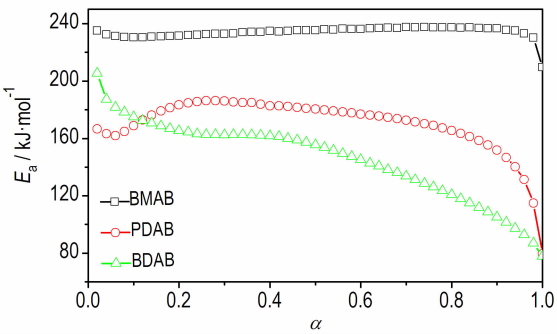

Fig. 3 E_a/α curves for the decomposition reaction of DMAB, PDAB and BDAB by Ozawa's method

Forty-one types of kinetic model functions and the basic data in Table 4 of DMAB, PDAB and BDAB are put into the integral and differential equations for calculation, the values of E_a, lg$A$, and linear correlation coefficient (r) are calculated with the linear least-squares method, and the most probable mechanism function is selected by the better value of r[26]. The results of satisfying the conditions at the same time are the final results as listed in Table 5, and the relevant function is the reaction mechanism function of the decomposition process.

Table 4 Thermal decomposition data determined by DSC curves at different heating rates for DMAB, PDAB and BDAB K

α	DMAB				PDAB				BDAB			
	T_5	T_{10}	T_{15}	T_{20}	T_5	T_{10}	T_{15}	T_{20}	T_5	T_{10}	T_{15}	T_{20}
0.02	570.96	577.53	583.15	586.32	510.78	522.81	523.83	528.12	521.33	527.84	533.04	536.70
0.06	579.19	586.65	592.08	595.40	515.27	526.60	529.59	533.93	524.60	532.42	537.95	541.68
0.10	583.14	590.93	596.24	599.69	517.79	528.02	531.67	535.97	526.37	534.68	540.42	544.25
0.14	585.66	593.61	598.87	602.35	519.38	528.82	532.77	536.90	527.65	536.28	542.18	546.08
0.18	587.50	595.55	600.75	604.28	520.37	529.29	533.43	537.44	528.69	537.57	543.63	547.63
0.22	588.95	596.98	602.23	605.77	521.05	529.61	533.86	537.84	529.65	538.68	544.88	548.93
0.26	590.15	598.28	603.43	607.00	521.51	529.87	534.19	538.20	530.42	539.68	546.01	549.93
0.30	591.17	599.34	604.47	608.09	521.81	530.13	534.49	538.55	531.18	540.62	546.87	550.79
0.34	592.07	600.26	605.37	608.95	522.04	530.37	534.75	538.90	531.90	541.45	547.60	551.55
0.38	592.87	600.99	606.16	609.77	522.26	530.63	535.03	539.25	532.58	542.10	548.29	552.39
0.42	593.59	601.79	606.92	610.52	522.49	530.90	535.32	539.62	533.22	542.67	549.00	553.20
0.46	594.29	602.47	607.59	611.19	522.71	531.20	535.62	539.99	533.76	543.23	549.71	554.10
0.50	594.90	603.16	608.23	611.86	522.96	531.50	535.92	540.38	534.21	543.78	550.47	555.06
0.54	595.51	603.77	608.86	612.47	523.23	531.84	536.26	540.79	534.60	544.37	551.29	556.03
0.58	596.09	604.35	609.41	613.05	523.50	532.20	536.61	541.25	534.99	544.99	552.16	557.08
0.62	596.67	604.94	610.02	613.63	523.81	532.62	536.99	541.76	535.40	545.66	553.10	558.27
0.66	597.23	605.49	610.59	614.17	524.16	533.08	537.43	542.33	535.83	546.40	554.12	559.52
0.70	597.79	606.08	611.16	614.74	524.58	533.62	537.89	543.02	536.31	547.18	555.28	560.93
0.74	598.35	606.65	611.73	615.34	525.04	534.26	538.46	543.83	536.83	548.11	556.57	562.50
0.78	598.93	607.26	612.36	615.95	525.63	535.04	539.12	544.85	537.43	549.13	558.05	564.30
0.82	599.57	607.91	613.02	616.65	526.36	536.03	539.93	546.16	538.14	550.35	559.82	566.43
0.86	600.26	608.66	613.78	617.39	527.33	537.30	540.96	547.88	539.01	551.84	561.91	568.98
0.90	601.11	609.54	614.67	618.32	528.67	539.05	542.31	550.33	540.16	553.75	564.63	572.26
0.94	602.17	610.75	615.91	619.55	530.68	541.75	544.24	554.28	541.82	556.46	568.50	576.87
0.98	604.22	613.17	618.37	622.12	534.23	546.80	547.62	562.82	545.11	561.44	575.29	585.11
1.00	612.57	624.55	628.10	633.01	541.71	554.86	550.67	578.15	554.66	572.23	588.48	601.36

Note: T with the subscript of 5, 10, 15 and 20 is the temperature obtained at the heating rate of 5.0, 10.0, 15.0, 20.0 K · min^{-1}, respectively.

From Table 5, one can find that the values of E_a and lg$A$ obtained from the nonisothermal DSC curves are in approximately good agreement with the values calculated by Kissinger's method and Ozawa's method, and the mechanism function number are determinated. Respectively substituting $f(\alpha)$ expression, the values of E_a/kJ·mol^{-1} and A/s^{-1} into Eq.(1)

$$d\alpha/dt = Af(\alpha)e^{-E/RT} \quad (1)$$

the following kinetic equations describing the main thermal decomposition process:

for DMAB,

$$d\alpha = 10^{18.02} \times 5(1-\alpha)[-\ln(1-\alpha)]^{3/5}/2 \times \exp(2.30 \times 10^5/RT)$$

for PDAB,

$$d\alpha = 10^{16.23} \times 4\alpha^{3/4} \times \exp(-1.85 \times 10^5/RT)$$

for BDAB,

$$d\alpha = 10^{16.58} \times 5(1-\alpha)[-\ln(1-\alpha)]^{3/5}/2 \times \exp(-1.93 \times 10^5/RT)$$

are obtained.

Table 5 Kinetic parameters for the main exothermic decomposition process of DMAB, PDAB and BDAB

method	β /K·min^{-1}	DMAB E_a /kJ·mol^{-1}	DMAB lg(A/s^{-1})	DMAB r	PDAB E_a /kJ·mol^{-1}	PDAB lg(A/s^{-1})	PDAB r	BDAB E_a /kJ·mol^{-1}	BDAB lg(A/s^{-1})	BDAB r
General integral	5.0	232.54	18.18	0.9999	199.09	17.69	0.9982	195.23	16.88	0.9999
	10.0	226.80	17.69	0.9998	176.48	15.39	0.9989	192.48	16.50	0.9999
	15.0	226.03	17.63	0.9998	169.67	14.74	0.9994	193.23	16.59	0.9997
	20.0	234.95	18.41	0.9996	193.02	17.06	0.9995	189.69	16.23	0.9998
Mac Callum-Tanner	5.0	235.57	18.49	0.9999	200.60	17.82	0.9983	196.86	17.02	0.9999
	10.0	229.92	17.99	0.9998	177.97	15.50	0.9990	194.07	16.76	0.9999
	15.0	229.23	17.94	0.9999	171.19	14.85	0.9995	195.11	16.75	0.9997
	20.0	238.28	18.74	0.9996	194.78	17.21	0.9996	191.60	16.39	0.9998
Šatava-Šesták	5.0	230.60	18.01	0.9999	197.59	17.54	0.9983	194.06	16.76	0.9999
	10.0	225.27	17.55	0.9998	176.22	15.35	0.9990	192.81	16.55	0.9999
	15.0	224.62	17.50	0.9999	169.82	14.73	0.9995	192.40	16.49	0.9997
	20.0	233.16	18.25	0.9996	192.08	16.96	0.9996	189.09	16.16	0.9998
Agrawal	5.0	232.54	18.18	0.9999	199.09	17.69	0.9982	195.23	16.88	0.9999
	10.0	226.80	17.69	0.9999	176.48	15.39	0.9989	192.48	16.50	0.9999
	15.0	226.03	17.63	0.9998	169.67	14.73	0.9994	193.23	16.59	0.9997
	20.0	234.95	18.41	0.9996	193.01	17.06	0.9995	189.69	16.23	0.9998
mean		230.46	18.02		184.80	16.23		192.95	16.58	
Flynn-Wall-Ozawa		243.52		0.9999	189.45		0.9999	192.50		0.9999
		228.85(T_e)		0.9999	206.22(T_e)		0.9998	229.02(T_e)		0.9991
Kissinger		246.02	19.35	0.9999	190.41	16.89	0.9999	195.23	16.88	0.9999

Because of the value of E_a for DMAB is the highest one, it can be deduced the thermal stability of DMAB is better than that of the others.

3.3 Thermal Safety

The values (T_{e0} and T_{p0}) of the initial temperature point at which DSC curve deviates from the onset temperature (T_e) and peak temperature (T_p) corresponding to $\beta \to 0$ are obtained by Eq.(2) (where b, c and d are coefficients), and the self-accelerating decomposition temperature (T_{SADT}) is obtainedby Eq.(3)[26-27]. The results are listed in Table 6.

$$T_{e(or\ p)\,i} = T_{e0(or\ p0)\,i} + b\beta_i + c\beta_i^2 + d\beta_i^3 \quad (2)$$

$$T_{SADT} = T_{e0} \quad (3)$$

The thermal ignition temperature (T_{be0} or T_{TIT}) is obtained by substituting E_{eO} and T_{e0} into Zhang-Hu-Xie-Li equation Eq.(4)[26], and the critical temperatures of thermal explosion (T_{p0} or T_b) is obtained by substituting E_{pO} and T_{p0} into the equation. The high value of T_b for DMAB (Table 6) illustrates the process of transition from thermal decomposition to thermal explosion is not easy to take palce.

$$T_{be0\ (or\ bp0)} = \frac{E_O - \sqrt{E_O^2 - 4E_O RT_{e0\ (or\ p0)}}}{2R} \quad (4)$$

The adiabatic time-to-explosion (t_{TIAD}) of energetic materials (EMs) is the time of decomposition transiting to explosion under the adiabatic conditions, which is also an important parameter for assessing the thermal stability and safety.

Substituting the following data

for DMAB: $c_p = 2.589 - 1.385 \times 10^{-2}T + 3.354 \times 10^{-5}T^2$, $E = 246.02 \times 10^3$ J·mol^{-1}, $A = 10^{19.35}$ s^{-1}, $Q = \Delta H = 1194.0$ J·g^{-1}, $T = T_b = 601.93$ K, $T_0 = T_{e0} = 576.87$ K, mechanism function: $f(\alpha) = 5(1-\alpha)[-\ln(1-\alpha)]^{3/5}/2$

for PDAB: $c_p = -0.2813 + 5.365 \times 10^{-3}T - 2.993 \times 10^{-7}T^2$, $E = 190.41 \times 10^3$ J·mol^{-1}, $A = 10^{16.89}$ s^{-1}, $Q = \Delta H = 620.35$ J·g^{-1}, $T = T_b = 524.66$ K, $T_0 = T_{e0} = 511.90$ K, mechanism function: $f(\alpha) = 4\alpha^{3/4}$

for BDAB: $c_p = 0.9018 - 2.297 \times 10^{-3}T + 1.239 \times 10^{-5}T^2$,

$E=193.41\times10^3$ J·mol^{-1}, $A=10^{16.73}$ s^{-1}, $Q=\Delta H=635.10$ J·g^{-1}, $T=T_b=536.73$ K, $T_0=T_{e0}=521.55$ K, mechanism function: $f(\alpha)=5(1-\alpha)[-\ln(1-\alpha)]^{3/5}/2$

into Smith equation Eq. (5) and Eq. (6)[27-29]

$$\alpha=\frac{1}{Q_d A}\int_{T_0}^{T}\frac{c_p}{Q_d}\mathrm{d}T \tag{5}$$

$$t_{TIAD}=\int_0^t \mathrm{d}t=\frac{1}{Q_d A}\int_{T_0}^{T}\frac{c_p\exp(E/RT)}{f(\alpha)}\mathrm{d}T \tag{6}$$

the values of t_{TIAD} for three salts are acquired and listed in Table 6.

It should be pointed out that the value of several parameters expect for T_d (There are water molecular in DMAB, and H_2O lost from the structure when the compound is heated from the room temperature) lines with the similar order, that is, BTATz>DMAB>BDAB>PDAB, which is in consistent with the result of E_a. Therefore, it can be predicted that the order of the thermal safety is as following: BTATz>DMAB>BDAB>PDAB.

Another valuable finding is the content of N has the affection to the thermal safety, and the thermal safety increases with the content of N growing.

Table 6 The thermal safty and thermodynamic properties of DMAB, PDAB and BDAB

salt	T_d /K	T_{SADT} /K	T_{TIT} /K	T_b /K	t_{TIAD} /s	$\Delta S^{\neq}$ /J·mol^{-1}·K^{-1}	$\Delta H^{\neq}$ /kJ·mol^{-1}	$\Delta G^{\neq}$ /kJ·mol^{-1}
DMAB	498.35	576.87	589.49	601.93	65.41	111.54	241.12	175.36
PDAB	530.05	511.90	522.92	524.66	24.80	65.61	186.15	152.52
BDAB	542.77	521.55	531.82	536.73	36.97	62.36	189.05	156.36
BTATz	598.65	559.28	572.76	585.30	83.38	131.83	244.24	167.57

Note: T_d is thermal degradation temperature, T_{SADT} is self-accelerating decomposition temperature, T_{TIT} is thermal ignition temperature, T_b is critical temperatures of thermal explosion temperature, t_{TIAD} is adiabatic time-to-explosion temperature, $\Delta S^{\neq}$ is entropy of activation, $\Delta H^{\neq}$ is enthalpy of activation, $\Delta G^{\neq}$ is free energy of activation.

3.4 Thermodynamic Properties of BTATz, DMAB, PDAB and BDAB

The entropy of activation ($\Delta S^{\neq}$), enthalpy of activation ($\Delta H^{\neq}$), and free energy of activation ($\Delta G^{\neq}$) of the main exothermic decomposition reaction, are obtained by Eqs. (7)-(9) with $T=T_{p0}$, $E=E_K$, and $A=A_K$[15, 25, 27-28], and also summarized in Table 6. The positive values of $\Delta G^{\neq}$ indicates that the exothermic decomposition reaction can proceed under the heating condition.

$$A\exp-\frac{E_a}{RT}=\frac{k_B T}{h}\exp-\frac{\Delta G^{\neq}}{RT} \tag{7}$$

$$\Delta H^{\neq}=E_a-RT \tag{8}$$

$$\Delta G^{\neq}=\Delta H^{\neq}-T\Delta S^{\neq} \tag{9}$$

Where h is the plank constant (6.625×10^{-34} J·s); k_B is the Boltzmann constant (1.3807×10^{-23} J·K^{-1})

3.5 Detonation Velocity and Detonation Pressure of PDAB

The detonation velocity (D) and detonation pressure (p) are the important targets of scaling the detonation characteristics of energetic materials, which can be predicted with the nitrogen equivalent equation (NE equation) shown as formulas (10)-(12)[30].

$$\sum N=\sum x_i N_i/M \tag{10}$$

$$D=(690+1160\rho_0)\sum N \tag{11}$$

$$p=1.092(\rho_0\sum N)^2-0.574 \tag{12}$$

Where ρ_0 represents the density of an explosive, g·cm^{-3}, $\sum N$ represents the total nitrogen equivalent of detonation product, N_i is the nitrogen equivalent value of the certain product, x_i is the mole number of certain detonation product produced by a mole explosive.

Table 7 Nitrogen equivalents of different detonation products

donation product	N_2	H_2O	CO	CO_2	O_2	C	H_2
nitrogen equivalent value	1.00	0.54	0.78	1.35	0.50	0.15	0.29

According to the order of H_2—CO—C in forming detonation products, the detonation products are determined as $C_7H_{20}N_{16}=10H_2+7C+8N_2$

Through the nitrogen equivalent indexes of the detonation products in Table 7 with $M=328$, $\rho_0=1.504$ g·cm^{-3}, total nitrogen equivalents of PDAB are obtained

$$\sum N=100\times(10\times0.29+7\times0.15+8\times1)/328=3.64$$

Based on the Eqs. (11) and (12), the values of D and p for PDAB were obtained as 8862.09 m·s^{-1} and 32.15 GPa, respectively.

4 Conclusions

(1) Three novel energetic salts of BTATz, DMAB, BDAB and PDAB, were synthesized and characterized. The Crystal structure of PDAB is monoclinic, space group $C2/c$. Moreover, many different hydrogen bonds existed in one unit of PDAB make the thermal stability of PDAB molecule increase.

(2) The density, decomposition temperature, detonation velocity and detonation pressure of PDAB are 1.504 g·cm^{-3}, 530.05 K, 8862.09 m·s^{-1} and 32.15 GPa, respectively.

(3) Using T_{SADT} as criterion, the heat-resisstance ability of three energetic salts of BTATz decreases in the order of DMAB (576.87 K)>BDAB(521.55 K)>PDAB(511.90 K).

(4) The thermal stability of BTATz, DMAB, PDAB and BDAB decreses in the order of BTATz>DMAB>BDAB>PDAB.

References:

[1] Hickey M A, Chavez D E, Naud D. Preparation of 3,3′-azobis (6-amino-1,2,4,5-tetrazine): United States, US6342589[P]. 2002.

[2] Hickey M A, Chavez D E, Naud D. 3,6-bis(1*H*-1,2,3,4-tetrazol-5-ylamino)-1,2,4,5-tetrazine or salt thereof: United States, US6657059[P]. 2003.

[3] YUE Sou-ti, YANG Shi-qing. Synthesis and properties of 3,6-bis (1*H*-1,2,3,4-tetrazol-5-yl-amino)-1,2,4,5-tetrazine[J]. *Chinese Journal of Energetic Material*(*Hanneng Cailiao*), 2004, 12 (3): 155–157.

[4] WANG Bo-zhou, LAI Wei-peng, LIU Qian, et al. Synthesis, characterization and quantum chemistry study on 3,6-bis(1*H*-1, 2,3,4-tetrazol-5-yl-amino)-1,2,4,5-tetrazine[J]. *Chinese Journal of Organic Chemistry*, 2008, 28(3): 422–427.

[5] Saikia A, Sivabalan R, Polke B G, et al. Burn rate measurements of HMX, TATB, DHT, DAAF, and BTATz[J]. *Journal of Hazardous Materials*, 2009, 170(1): 306–311.

[6] ZHANG Xing-gao, ZHU Hui, YANG Shi-qing, et al. Study on thermal decomposition kinetics and mechanism of nitrogen-rich compound BTATz[J]. *Journal of Propulsion Technololgy*, 2007, 28(3): 322–325.

[7] Chavez D E, Hickey M A, Naud D. Tetrazine Exposives[J]. *Propellants, Explosives, Pyrotechnics*, 2004, 29(4): 209–215.

[8] Son S F, Berghout H L, Bolme C A. Burn rate measurements of HMX, TATB, DHT, DAAF, and BTATz[J]. *Proceeding of the Combustion Institute*, 2000, 28(1): 919–924.

[9] LI Na, ZHAO Feng-qi, LUO Yang, et al. Dissolution properties of 3,6-bis(1*H*-1,2,3,4-tetrazol-5-yl-amino)-1,2,4,5-tetrazine in N-methyl pyrrolidone and dimethyl sulfoxide[J]. *Journal of Solution Chemistry*, 2014, 43(7): 1250–1258.

[10] ZHANG Xian-bo, REN Ying-hui, LI Wen, et al. A novel magnesium salt based on BTATz: crystal structure, thermal behavior and thermal safety[J]. *Chemical Research in Chinese Universities*, 2013, 29(4): 627–631.

[11] ZHANG Xian-bo, REN Ying-hui, LI Wen, et al. 3,6-Bis(1*H*-1, 2,3,4-tetrazol-5-yl-amino)-1,2,4,5-tetrazine-based energetic strontium (Ⅱ) complexes: synthesis, crystal structure and thermal properties[J]. *Journal of Coordination Chemistry*, 2013, 66: 2051–2064.

[12] LI Wen, REN Ying-hui, ZHAO Feng-qi, et al. Nitrogen-rich energetic zinc salt on BTATz: syntheses and thermodynamic[J]. *Journal of Functional Materials*, 2013, 44(22): 3326–3329.

[13] LI Wen, REN Ying-hui, ZHAO Feng-qi, et al. Effects of lead complex-based BTATz on thermal behaviors, non-isothermal reaction kinetics and combustion properties of DB/RDX-CMDB propellants[J]. *Acta Physico-Chimica Sinica*, 2013, 29(10): 2087–2094.

[14] REN Ying-hui, LI Wen, ZHANG Xian-bo, et al. Nonisothermal decomposition kinetics and thermal safety of Ag_2(BTATz)·2H_2O(BTATz=3,6-bis(1*H*-1,2,3,4-tetrazole-5-amino)-1,2,4,5-tetrazine)[J]. *Journal of Applied Chemisty*, 2013, 30(9): 1036–1041.

[15] YI Jian-hua, ZHAO Feng-qi, WANG Bo-zhou, et al. Thermal behaviors, non-isothermal decomposition reaction kinetics, thermal safety and burning rates of BTATz-CMDB propellant [J]. *Journal of Hazardous Materials*, 2010, 181: 432–439.

[16] YI Jian-hua, ZHAO Feng-qi, WANG Bo-zhou, et al. BTATz-HNIW-CMDB propellants decomposition reaction kinetics and thermal safety[J]. *Journal of Thermal Analysis and Calorimetry*, 2014, 115(2): 1227–1234.

[17] Hickey M A, Chavez D E, Naud D. Low-smoke pyrotechnic compositions: United States, US6312537[P]. 2001.

[18] LI Shang-wen, ZHAO Feng-qi, YUAN Chao. Tendency of research and development for overseas solid propellants[J]. *Journal of Solid Rocket Technology*, 2002, 25(2): 36–42.

[19] Hickey M A, Chavez D E, Naud D. Propellant containing 3,6-bis(1*H*-1,2,3,4-tetrazol-5-yl-amino)-1,2,4,5-tetrazine or salts thereof. US 6458227[P]. 2002.

[20] Wang R H, Xu H Y, Guo Y. et al. Bis[3-(5-nitroimino-1,2,4-triazolate)]-based energetic salts: synthesis and promising properties of a new family of high-density insensitive materials[J]. *Journal of the American Chemical Society*, 2010, 132 : 11904–11905.

[21] BI Fu-qiang, FAN Xue-zhong, Xu Cheng, et al. Review on insensitive non-metallic energetic ionic compounds of tetrazolate anions[J]. *Chinese Journal of Energetic Materials*(*Hanneng Cailiao*), 2012, 20(6): 805–811.

[22] ZHAI Lian-jie, FAN Xue-zhong, WANG Bo-zhou, et al. Synthesis and properties of 5-(3-amino-1,2,5-oxadiazol-4-yl) tetrazol-1-ol and its ammonium and hydroxylammonium salts[J]. *Chinese Journal of Energetic Materials*(*Hanneng Cailiao*), 2016, 24 (9): 862–867.

[23] LI Hui, YU Qian-qian, WANG Bo-zhou, et al. Synthesis and properties of 3,3′-bis (tetrazol-5-yl)-4,4′-azofurazan and its energetic salts[J]. *Chinese Journal of Energetic Materials*(*Hanneng Cailiao*), 2013, 21(6): 821–824.

[24] Sheldric G M. SHELXL-97, Program for the refinement of crystal structure[CP], University of Gottingen, Germany 1997.

[25] YI Jian-hua, ZHAO Feng-qi, GAO Hong-xu, et al. Preparation, characterization, nonisothermal reaction kinetics, thermodynamic properties, and safety performances of high nitrogen compound: hydrazine 3-nitro-1,2,4-triazol-5-one complex[J]. *Journal of Hazardous Materials*, 2008, 153: 261–268

[26] HU Rong-zu, GAO Sheng-li, ZHAO Feng-qi, et al. Thermal analysis kinetics (2th)[M]. Science Press, Beijing, 2008: 151–155.

[27] ZHAOFeng-qi, HU Rong-zu, GAO Hong-xu, et al. New developments in hazardous materials research[M]. Nova Science Publishers Inc., New York, 2006: 161–167.

[28] REN Ying-hui, ZHAO Feng-qi, YI Jian-hua, et al. Studies on an ionic compound (3-ATz)$^+$(NTO)$^-$: crystal structure, specific heat capacity, thermal behaviors and thermal safety[J]. *Journal of Iranian Chemical Society*, 2012, 9: 407–414.

[29] REN Ying-hui, LI Wen, ZHAO Feng-qi, et al. Crystal structure and thermal behaviors for 3,5-dinitrobenzoic acid of 3,5-diami-

no-1,2,4-triazole[J]. *Journal of Analytical and Applied Pyrolysis*, 2013, 102: 89-96.
[30] CHEN Hua-xiong, CHEN Shu-sen, LI Li-jie, et al. Synthesis, single crystal structure and characterization of pentanitromonoformylhexaazaisowurtzitane[J]. *Journal of Hazardous Materials*, 2010, 175(1-3): 569-574

3,6-双(1-氢-1,2,3,4-四唑-5-氨基)-*s*-四嗪(BTATz)含能离子盐的合成与性能

刘 晴[1], 杨 瑾[1], 任莹辉[1], 马海霞[1], 徐抗震[1], 张 超[1], 赵凤起[2], 胡荣祖[2]
(1. 西北大学化工学院, 陕西 西安 710069; 2. 西安近代化学研究所, 陕西 西安 710065)

摘 要: 合成了三种基于3,6-双(1-氢-1,2,3,4-四唑-5-氨基)-*s*-四嗪(BTATz)的含能离子盐: 二甲胺盐(DMAB),1,3-丙二胺盐(PDAB)和1,4-丁二铵盐(BDAB)。用IR, ^{1}H NMR, ^{13}C NMR和元素分析表征了DMAB、PDAB和BDAB的结构。采用X-射线单晶衍射测定了PDAB的晶体结构。计算了PDAB的爆速(D)和爆压(p)。用DSC和TG-DTG研究了DMAB、PDAB和BDAB的热分解行为。计算了自加速分解温度(T_{SADT}),热爆炸临界温度(T_b),热点火温度(T_{TIT})及绝热至爆时间(t_{TIAD})。结果表明, PDAB晶体属于单斜晶系, $C2/c$ 空间群, 晶胞参数: a=2.2699(10) nm, b=0.5098(2) nm, c=1.6449(6) nm, β=93.045(15)°, V=1.9008(13) nm^3, D_c=1.504 g·cm^{-3}, Z=4, $F(000)$=912, μ=0.127 mm^{-1}, R_1=0.0673, wR_2=0.2002。PDAB的爆速和爆压分别为8862.09 m·s^{-1}和32.15 GPa。DMAB、PDAB和BDAB的T_{SADT}值分别为576.87,511.90,521.55 K,显示DMAB的热稳定性优于PDAB和BDAB。DMAB、PDAB和BDAB均可作为潜在的含能材料且DMAB的性能优于PDAB和BDAB。

关键词: 3,6-双(1-氢-1,2,3,4-四唑-5-氨基)-*s*-四嗪(BTATz); 离子盐; 热分解行为; 热安全性
中图分类号: TJ55 **文献标志码:** A **DOI:** 10.11943/j.issn.1006-9941.2017.07.007